Analysis of Noncharacteristic Harmonics Generated by Voltage-Source Converters Operating Under Unbalanced Voltage

Claudionor F. Nascimento, Edson H. Watanabe, *Senior Member, IEEE*, Oumar Diene, Alvaro B. Dietrich, Alessandro Goedtel, Johan J. C. Gyselinck, and Robson F. S. Dias

***Abstract*—This paper deals with an analytical model to evaluate the noncharacteristic harmonics that are generated by three-phase three-wire voltage-source converters (VSCs) operating under unbalanced sinusoidal voltage conditions. This model permits the calculation of the oscillating current on the VSC dc side by considering the unbalanced voltages on its ac side. It can be used to prove that the use of dc voltage control techniques to eliminate VSC dc-side double frequency voltage ripple necessarily creates three-phase currents with undesirable low-frequency harmonic components on the VSC ac side. In this paper, the attention is directed to the instantaneous oscillating real power component at twice the line frequency, rather than to other power components. The noncharacteristic current components analyzed in this paper, such as the fundamental negative sequence and third-order harmonic components of positive and negative sequences are calculated using the proposed model in time-domain simulations. A simple model to calculate the dc-side capacitor to mitigate these noncharacteristic harmonic problems is presented.**

***Index Terms*—Noncharacteristic harmonics, renewable energy source, STATCOM, VSC inertia constant.**

NOMENCLATURE

C	VSC dc-side capacitance.
H_c	VSC inertia constant.
I_+	RMS value of the positive-sequence current component.
I_{a+}, I_{a-}	RMS values of the fundamental positive- and negative-sequence current components.
I_{a3+}, I_{a3-}	RMS values of the third-order positive- and negative-sequence current components.
$I_s, \tilde{i}_s$	VSC dc-side external source average and oscillating current components.
i_a, i_b, i_c	VSC ac terminal currents.
i_d	VSC dc capacitor instantaneous current.
i_{dc}	VSC dc terminal current.
i_s	VSC dc-side external source instantaneous current.
PCC	Point of common coupling.
p, q	VSC ac terminal instantaneous real and imaginary power.
$\overline{p}, \tilde{p}$	VSC ac terminal average and oscillating power components.
$\overline{p}_{dc}, \tilde{p}_{dc}$	VSC dc terminal average and oscillating power components.
p_s	VSC dc-side external source power.
THD	Total harmonic distortion.
V_+, V_-	RMS values of the positive- and negative- sequence voltage components at PCC.
$V_{dc}, \tilde{v}_{dc}$	VSC dc-side average and voltage ripple components.
VSC	Voltage-source converter.
v_a, v_b, v_c	AC voltages at PCC.
v_{dc}	VSC dc terminal instantaneous voltage.
ΔV_{dc}	VSC dc-side peak-to-peak voltage ripple.
δ	Unbalance factor of the voltage at PCC.
ε	VSC dc-side ripple voltage factor.
ϕ_{i_+}	Phase angle of current positive-sequence.
ϕ_{v_+}, ϕ_{v_-}	Phase angles of the positive- and negative- sequence voltage components.
ω	Grid angular frequency.

Manuscript received December 15, 2015; revised April 30, 2016 and July 20, 2016; accepted July 9, 2016. Date of publication July 20, 2016; date of current version March 22, 2017. This work was supported in part by FAPESP under Grant 2014/14361-8; in part by CNPq under Grants 306243/2014-8, 552269/2011-5, and 311558/2015-1; and in part by FAPERJ under Grants E-26/201.223/2014, E-26/101.953/2012, and E-26/110.400/2014. Paper no. TPWRD-01790-2015.

C. F. Nascimento is with CCET, Universidade Federal de São Carlos, São Carlos, C. P. 676, Brazil (e-mail: claudionor@ufscar.br).

E. H. Watanabe is with COPPE, Universidade Federal do Rio de Janeiro, Rio de Janeiro, Brazil (e-mail: watanabe@coe.ufrj.br).

O. Diene and R. F. S. Dias are with COPPE and Poli, Universidade Federal do Rio de Janeiro, Rio de Janeiro, Brazil (e-mail: oumar@dee.ufrj.br).

A. B. Dietrich is with CECS, Universidade Federal do ABC, Santo André, Brazil (e-mail: alvaro.dietrich@ufabc.edu.br).

A. Goedtel is with DEE, Universidade Tecnológica Federal do Paraná, Cornélio Procópio, Brazil (e-mail: agoedtel@utfpr.edu.br).

J. J. C. Gyselinck is with BEAMS, Université Libre de Bruxelles, Brussels, Belgium (e-mail: johan.gyselinck@ulb.ac.be).

Color versions of one or more of the figures in this paper are available online at http://ieeexplore.ieee.org.

Digital Object Identifier 10.1109/TPWRD.2016.2593684

I. INTRODUCTION

VOLTAGE-SOURCE converters (VSCs) are widespread in industrial, commercial, and home applications. The three-phase three-wire VSC configuration is widely used to constitute these applications. These converters have some interesting features reported in the literature, such as independent control of instantaneous active and reactive power delivered [1], and bidirectional power flow [2].

During the last decade the penetration of alternative renewable energy sources (e.g., wind and solar [3]) connected to the

grid has increased significantly in several countries around the world. This growth is due to the global concern about sustainability regarding electrical energy generation/consumption and it was made viable by the development of new power electronic equipment such as VSCs. These converters can be also used as compensators for voltage control like STATCOM [4], as a rectifier [2], and as a modular multilevel converter (MMC) [1].

In general, VSCs are also subject to power quality disturbances such as unbalanced voltages. The study of converters operating under unbalanced voltage condition (as studied in [5] and [6]) is essential, since it is a common issue in relatively weak systems, where single-phase loads are predominant. The occurrence of voltage unbalance causes disturbances, such as torque ripple in induction generators, reduction of lifetime and reliability of VSC dc-side capacitors [7]. This occurs because the voltage unbalance may result in excess of dc voltage ripple on the dc-side of three-phase VSC, as confirmed in [8].

The authors of [9] discussed the influence of the oscillating power components caused by unbalanced voltages and currents at the point of common coupling (PCC) of a power system. The behavior on the dc side of a VSC subject to unbalanced ac voltage investigated in [4] and [6] demonstrated that a voltage ripple with frequency equivalent to 2ω (ω being the grid frequency) appears on this dc voltage. However, there is no detailed analytical study in the literature about the magnitude of this voltage ripple, i.e., although this ripple with frequency 2ω is well known [6], it was not quantified in relation to the negative-sequence component.

The VSC dc-side voltage ripple generates harmonics on its ac-side currents. The authors of [5] mention that unbalanced voltage is responsible for noncharacteristic third-order harmonic current generation on the VSC ac side, but they do not present quantitative analysis of this phenomenon. In [1], the authors have also studied the effects of unbalanced voltage in the ac current and the submodule (one half-bridge module) capacitor voltage, however they do not show the amplitude of the current harmonic components on the VSC.

For the analysis in this work, the noncharacteristic harmonic components are considered as the steady state low-frequency harmonic components, which may be present in the voltage or current and would not appear if the grid voltage were balanced. This includes the fundamental frequency negative-sequence component and the positive-sequence third-order harmonic.

The noncharacteristic third-order positive-sequence harmonic cannot be eliminated by transformers with windings connected in delta. On the other hand, the conventional characteristic third-order harmonics are generally of zero-sequence component type and can be eliminated by using transformers. Therefore, this third-order positive-sequence component deserves special attention.

In order to eliminate the dc oscillating voltage when the ac-side voltage is unbalanced, the athors of [6] proposed a VSC dc-side voltage controller, which its dynamics are modeled as two decoupled subsystems. However, the side effects of the proposed control over the ac-side current are not considered in their work [6]. It is important to analyze what happens when a VSC is controlled in such a way that the oscillating voltage across the dc capacitor is eliminated, because this operating condition leads to unbalanced and distorted ac-side currents.

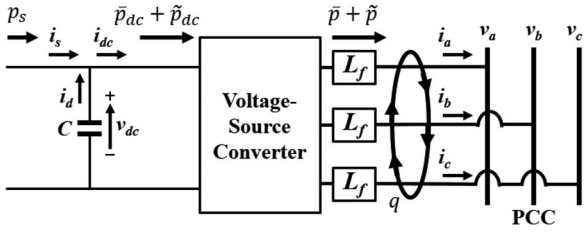

Fig. 1. VSC connected to the ac grid.

In a previous paper [8] with other results of this work, we have presented a quantitative study about noncharacteristic harmonic generation due to unbalanced voltage, considering the presence of oscillating power on the dc- and ac-side of the VSC. A simple and precise formulation was presented to calculate the VSC dc-side capacitance in order to mitigate characteristic and noncharacteristic harmonic components, as shown in [8].

In this present work, we analyze and quantify the influence of VSC dc side voltage ripple on its ac side. It is shown that low order noncharacteristic current harmonics appears on the ac side. Also, this work shows that if a VSC is controlled to eliminate dc voltage ripple [6], when connected to an unbalanced three-phase voltage, the VSC has to operate with constant ac power control, i.e., without oscillating power at VSC dc and ac sides. In this case, the ac-side currents of the converter necessarily contain undesirable noncharacteristic low-frequency components such as the fundamental negative-sequence and third-order harmonic components of positive and negative sequences.

The validity of the proposed model is supported by numerical and time-domain simulations using PSCAD/EMTDC.

The assumptions made throughout this paper are listed as follows:

1) the VSC is designed to operate with pulse-width modulation (PWM)-based current control to inject balanced three-phase currents at the fundamental frequency in the grid when dc voltage is constant;
2) the harmonics due to the switching are completely eliminated by the ac series filter;
3) the VSC is a three-wire converter, therefore no zero-sequence current component exists on its ac side;
4) the negative-sequence voltage component present on the ac-side is due to the unbalanced load condition;
5) the VSC switching losses do not affect the VSC switching function, thus, for simplicity and without losing generality, it is assumed that the VSC is lossless;
6) the three-phase distribution system has balanced three-phase voltage source (v_{as}, v_{bs}, v_{cs}) at no-load condition;
7) the series VSC impedance (R_f and L_f) and the grid (R_s and L_s) impedance are linear and balanced.

II. Modeling the Voltage-Source Converter

The analysis and modeling of the three-phase three-wire VSC are presented based on Fig. 1, where the VSC can be a two-level bridge converter or a three-level neutral point clamped converter,

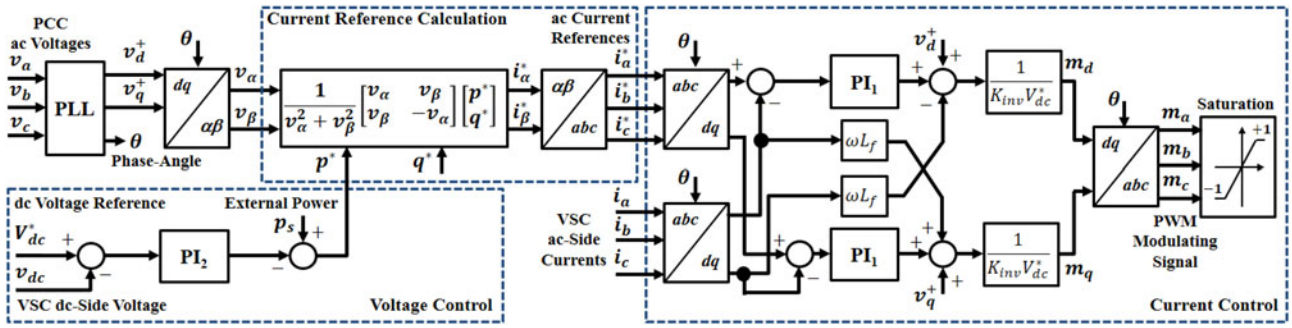

Fig. 2. VSC control system.

and the ac system is weak, but originally balanced. The analysis is based on instantaneous values of voltage and current.

In Fig. 1, the current i_{dc} is the total instantaneous current flowing to the VSC dc side, v_{dc} is the instantaneous voltage across the dc capacitor and i_d is the instantaneous current flowing in the dc capacitor. This dc capacitor is supposed to have a high quality factor; therefore, a zero equivalent series resistance is considered in the model. The instantaneous power p_s may be supplied by an external source, e.g., a solar panel or wind generator. The dc current i_s is the instantaneous current supplied by the external source, and is equal to zero when the VSC operates as a reactive power compensator (STATCOM). Here, for simplicity, it is assumed that there is no oscillating component on i_s. The oscillating power component on the VSC ac side $\tilde{p}$, its average component $\overline{p}$ and the imaginary power q are derived from the p-q Theory [9]. The instantaneous imaginary power q is proportional to the energy which is exchanged between the phases of the system (this fact is illustrated in Fig. 1 by the ellipse with arrows in the VSC ac side) [9]. The dc-side instantaneous power is divided into its average value $\overline{p}_{dc}$ and its oscillating component $\tilde{p}_{dc}$. The three-phase ac currents (i_a, i_b, i_c) flow through coupling inductance (L_f), while the ac voltages (v_a, v_b, v_c) at the PCC may be unbalanced due to the load configuration.

The block diagram of the VSC control system is depicted in Fig. 2. This control system consists of (i) a voltage control; (ii) a phase-locked loop (PLL) [6]; (iii) a function determining the current reference; and (iv) a current control. The instantaneous real power reference p^* is calculated by using the voltage proportional and integral controller PI_2, which considers the difference between the desired voltage V_{dc}^* and the instantaneous VSC dc terminal voltage v_{dc} as input. The instantaneous imaginary power reference q^* could be calculated to control the ac voltage or compensate for reactive power, but for simplicity, it is considered zero. The dq-frame is synchronized to the positive-sequence component of the ac voltage at PCC using a PLL, which transforms v_a, v_b, v_c to v_d^+ and $v_q^+ = 0$, and adjust $\theta = \omega t$ in the steady-state. Before using the p-q Theory [9] to determine the current references i_a^*, i_b^* and i_c^*, the dq-frame voltages are converted into the $\alpha\beta$-frame voltages v_α, v_β. The current references i_a^*, i_b^*, i_c^* are then obtained by a $\alpha\beta$- to abc-frame transformation. Using abc- to dq-frame transformation, the VSC ac terminal currents i_a, i_b, i_c are compared to the reference currents i_a^*, i_b^*, i_c^*, and regulated by a PWM switching strategy in order to inject balanced three-phase currents. In this work, all time-domain simulations are performed including the PWM switching. m_d and m_q in Fig. 2 denote, respectively, the d- and q-axis components of the PWM modulating signal m_a, m_b, m_c, and K_{inv} is the VSC low frequency gain.

A maximum power point tracking (MPPT) algorithm can be used to maximize the energy generated by an alternative renewable source (e.g., a photovoltaic source) connected to the ac grid through the VSC [10]. As mentioned above, the VSC analyzed in this work has a current control loop and, therefore, operates as a sinusoidal balanced current source, when the dc voltage is ripple-free, i.e. VSC operating condition with only average voltage on dc side, which allows for better control of the injected power into the distribution system.

A. Instantaneous Power Components on the VSC AC Side

In this subsection, the instantaneous power components on the VSC ac side due to unbalanced grid voltage are derived from the p-q Theory.

Each phase voltage at PCC (Fig. 1) can be represented considering positive- and negative-sequence components as follows:

$$\begin{cases} v_a = \sqrt{2}V_+ \sin(\omega t + \phi_{v_+}) + \sqrt{2}V_- \sin(\omega t + \phi_{v_-}) \\ v_b = \sqrt{2}V_+ \sin\left(\omega t + \phi_{v_+} - \dfrac{2\pi}{3}\right) + \sqrt{2}V_- \sin\left(\omega t + \phi_{v_-} + \dfrac{2\pi}{3}\right) \\ v_c = \sqrt{2}V_+ \sin\left(\omega t + \phi_{v_+} + \dfrac{2\pi}{3}\right) + \sqrt{2}V_- \sin\left(\omega t + \phi_{v_-} - \dfrac{2\pi}{3}\right) \end{cases} \tag{1}$$

where V_+ and V_- are the rms values of the positive- and negative-sequence voltage components, respectively, and ϕ_{v_+} and ϕ_{v_-} are the respective phase angles.

The three-phase currents supplied by the VSC, as shown in Fig. 1, for constant v_{dc}, are given by

$$\begin{cases} i_a = \sqrt{2}I_+ \sin(\omega t + \phi_{i_+}) \\ i_b = \sqrt{2}I_+ \sin\left(\omega t + \phi_{i_+} - \dfrac{2\pi}{3}\right) \\ i_c = \sqrt{2}I_+ \sin\left(\omega t + \phi_{i_+} + \dfrac{2\pi}{3}\right) \end{cases} \tag{2}$$

where I_+ is the rms value of the positive-sequence current component; ϕ_{i+} is the phase angle of this positive-sequence current with respect to positive-sequence voltage.

For the purpose of the analysis of the VSC under unbalanced voltage, as given in [11], the voltage unbalance factor δ is defined as the relation between positive- and negative-sequence

voltages, as follows:

$$\delta = \frac{V_-}{V_+}. \tag{3}$$

The average and oscillating components of real power ($p = \bar{p} + \tilde{p}$) and imaginary power ($q = \bar{q} + \tilde{q}$), as calculated by the authors in [8], at VSC ac terminals are given by

$$\begin{cases} \bar{p} = 3V_+ I_+ \cos(\phi_{v_+} - \phi_{i_+}) \\ \tilde{p} = -3V_- I_+ \cos(2\omega t + \phi_{v_-} + \phi_{i_+}) \\ \bar{q} = 3V_+ I_+ \sin(\phi_{v_+} - \phi_{i_+}) \\ \tilde{q} = 3V_- I_+ \sin(2\omega t + \phi_{v_-} + \phi_{i_+}). \end{cases} \tag{4}$$

These oscillating power components in (4) are due to the cross product of the negative-sequence voltage and the positive-sequence current, whereas the average components result from the interaction between the positive-sequence voltage and the positive-sequence current [8]. The imaginary power q does not cause any effect on the VSC dc side [9]. However, the average $\bar{p}$ and the oscillating component $\tilde{p}$ of the real power correspond to the energy exchanged between the dc- and the ac-sides of the VSC [9].

The focus of this work is directed to the oscillating power $\tilde{p}$, which occurs at twice the line frequency, rather than to other power components, such as the imaginary power q.

In general, the VSC dc-side voltage v_{dc} is supposed to be constant in the models found in literature. However, in practical applications, v_{dc} might contain some ripple, due to the switching, that can be eliminated by calculating correctly the dc-side capacitor. Furthermore, as said before, a 2ω voltage ripple may appear in this dc voltage due to ac-side oscillating power.

An analytical model for the case of the dc-voltage 2ω ripple elimination control, e.g. the one proposed in [6], is presented to prove that negative sequence fundamental component as well as the third-order positive sequence harmonic appears, and some power quality indices, like total harmonic distortion (THD) or third-order harmonic content, may be deteriorated.

B. Instantaneous Power Components on the VSC DC Side

In general, the VSC dc-side voltage is supposed to be constant but, in this paper, as said before, the focus is on the dc voltage and the current ripples created by the oscillating power component $\tilde{p}$, which is due to the unbalanced voltage on the VSC ac side. The instantaneous voltage v_{dc} across the dc-side capacitor C (Fig. 1) is considered as

$$v_{dc} = V_{dc} + \tilde{v}_{dc} \tag{5}$$

where V_{dc} is the average voltage component across the dc capacitor and $\tilde{v}_{dc}$ is the instantaneous dc voltage ripple.

The instantaneous real power on the VSC dc side is given by

$$p_{dc} = V_{dc} I_s + V_{dc} \tilde{i}_s + V_{dc} i_d + \tilde{v}_{dc} I_s + \tilde{v}_{dc} \tilde{i}_s + \tilde{v}_{dc} i_d \tag{6}$$

where $\tilde{i}_s$ and I_s are respectively the oscillating and average current components from the external source on the dc side of the VSC, and i_d is the dc capacitor current [8].

Assuming the instantaneous VSC dc- and ac-side power balance under no-loss condition ($p_{dc} = p$), the average and oscillating power components can be written as follows:

$$\begin{cases} \bar{p}_{dc} = \bar{p} = V_{dc} I_s = 3V_+ I_+ \cos(\phi_{v_+} - \phi_{i_+}) \\ \tilde{p}_{dc} = \tilde{p} = V_{dc} \tilde{i}_s + V_{dc} i_d + \tilde{v}_{dc} I_s + \tilde{v}_{dc} \tilde{i}_s + \tilde{v}_{dc} i_d \\ \qquad = -3V_- I_+ \cos(2\omega t + \phi_{v_-} + \phi_{i_+}). \end{cases} \tag{7}$$

This equation for $\tilde{p}_{dc}$ is very important and dictates how the dc capacitor voltage behaves in the presence of the negative-sequence voltage on the VSC ac side or the oscillating current coming from the alternative source. In this work, the analysis is restricted to the case when $\tilde{i}_s$ is negligible. There may be some oscillating current $\tilde{i}_s$, but here the oscillating frequency of this current is considered to be much lower than 2ω. This oscillating current component $\tilde{i}_s$ will be analyzed in future work.

III. Analysis of VSC Under Unbalanced Conditions

The VSC connected to the grid under unbalanced conditions, without the dc side source, i.e., operating as STATCOM (the current flowing from an external source in Fig. 1 is equal to zero, i.e. $i_s = 0$) or with an alternative renewable energy source ($i_s \neq 0$) connected on its dc side are analyzed in this section.

Ideally, the VSC operating as a shunt compensator should compensate for reactive power, working as a STATCOM. The authors of [12] present the compensating current references generated to compensate for the undesired components of q. The real average power component in the STATCOM is equal to zero ($\bar{p} = \bar{p}_{dc} = 0$), whereas the real oscillating power is different from zero ($\tilde{p} = \tilde{p}_{dc} = v_{dc} i_d$) [8]. However, the influence of the oscillating power components on the ac and dc sides of the VSC was not discussed in [12]. These oscillating power components were presented in [4], but without analytical study of the magnitude of the voltage ripple.

Considering that a renewable energy source (connected to the VSC dc side) supplies only constant average ac power when it is operating with an ideal MPPT, the average power component $\bar{p}$ from this VSC is controlled such that $\bar{p}_{dc} = V_{dc} I_s$, while the oscillating power $\bar{p}$, due to the unbalanced voltage, must be supplied or absorbed by the dc capacitor to satisfy the VSC dc- and ac-side power balance ($\tilde{p} = \tilde{p}_{dc} = v_{dc} i_d$) [8]. This situation represents a case in which all the VSC ac-side oscillating power must be balanced by the dc capacitor, similar to the case of a VSC operating as STATCOM.

Since the instantaneous power at the VSC dc-side capacitor C is $v_{dc} i_d = \tilde{p}$ for both VSC operating situations, either as STATCOM or inverter used for the connection of renewable energy sources to the grid, the instantaneous oscillating VSC dc-side power is given by

$$\tilde{p}_{dc} = v_{dc} i_d = -3V_- I_+ \cos(2\omega t + \phi_{v_-} + \phi_{i_+}). \tag{8}$$

The oscillating power given by (8) dictates the size of the VSC dc capacitance necessary to mitigate the voltage ripple caused by the negative-sequence voltage component. The authors of [13] show a method for dc capacitor calculation, but without calculating the oscillating power and the VSC dc-side current

ripple. Using (7) and (8), it can be written that:

$$V_{dc}C\frac{d\tilde{v}_{dc}}{dt}+\tilde{v}_{dc}C\frac{d\tilde{v}_{dc}}{dt}=-3V_{-}I_{+}\cos\left(2\omega t+\phi_{v_{-}}+\phi_{i_{+}}\right). \tag{9}$$

Solution for (9) using numerical calculations is given by

$$\tilde{v}_{dc}=-V_{dc}+\sqrt{V_{dc}^{2}+\gamma^{2}-\frac{3V_{-}I_{+}}{\omega C}\sin\left(2\omega t+\phi_{v_{-}}+\phi_{i_{+}}\right)} \tag{10}$$

where

$$\gamma=\frac{-3V_{-}I_{+}}{2\omega CV_{dc}}\sin\left(\phi_{v_{-}}+\phi_{i_{+}}\right). \tag{11}$$

However, it is possible to find a simplified solution for (9), assuming that the capacitor power is given by

$$v_{dc}i_{d}=\frac{dE_{c}}{dt}=\frac{d}{dt}\left(\frac{1}{2}Cv_{dc}^{2}\right), \tag{12}$$

where E_c is the energy stored in the capacitor C. Since the capacitor receives all oscillating energy from the ac oscillating power ($v_{dc}i_d=\tilde{p}$), as $i_s=0$ (e.g., a STATCOM) or $i_s=I_s$ ($\overline{p}_{dc}=V_{dc}I_s$), (12) can be rewritten as

$$\frac{1}{2}C\frac{d(V_{dc}+\tilde{v}_{dc})^{2}}{dt}=-3V_{-}I_{+}\cos\left(2\omega t+\phi_{v_{-}}+\phi_{i_{+}}\right). \tag{13}$$

If $\tilde{v}_{dc}$ is significantly smaller than V_{dc}, then $\tilde{v}_{dc}^2$ can be neglected when compared to V_{dc}^2 (i.e., $V_{dc}^2+2V_{dc}\tilde{v}_{dc}\gg\tilde{v}_{dc}^2$), which results in

$$\frac{d\tilde{v}_{dc}}{dt}\cong\frac{-3V_{-}I_{+}}{CV_{dc}}\cos\left(2\omega t+\phi_{v_{-}}+\phi_{i_{+}}\right). \tag{14}$$

Then, the integration of both sides of (14) leads to the dc voltage ripple at twice the line-frequency. Thus,

$$\tilde{v}_{dc}=\frac{3V_{-}I_{+}}{2\omega CV_{dc}}\sin\left(2\omega t+\phi_{v_{-}}+\phi_{i_{+}}+\pi\right). \tag{15}$$

The magnitude of the voltage ripple in (15) matches one of the ripple presented in [14]; however, the effects of negative-sequence are not presented in their work.

The peak-to-peak voltage ripple value ΔV_{dc} is defined by

$$\Delta V_{dc}=\frac{3V_{-}I_{+}}{\omega CV_{dc}}, \tag{16}$$

whereas, the dc capacitor ripple voltage factor ε is defined as

$$\varepsilon=\frac{\Delta V_{dc}}{V_{dc}}. \tag{17}$$

Therefore, $\tilde{v}_{dc}$ can be rewritten generically as

$$\tilde{v}_{dc}=\frac{\varepsilon V_{dc}}{2}\sin\left(2\omega t+\phi_{v_{-}}+\phi_{i_{+}}+\pi\right). \tag{18}$$

For a given ac voltage unbalance factor δ, dc capacitor ripple voltage factor ε, rated ac voltage, current and frequency and the dc voltage, the value of the capacitance C in the VSC dc-side under unbalanced conditions can be calculated by

$$C=\frac{3\delta V_{+}I_{+}}{\omega\varepsilon V_{dc}^{2}}. \tag{19}$$

Considering practical systems, the capacitance cannot be zero (i.e., the unbalance factor $\delta=0$; therefore, $C=0$) due to converter switching, which imposes energy variation to it, even if the renewable energy source on VSC dc side has no oscillation. The dc capacitance obtained using (19) is the capacitance that allows the VSC to operate with a given unbalance voltage factor δ and ripple voltage factor ε. At this point, it is interesting to mention the studies of [15] and [7], which have analyzed the ripple current stresses and lifetime models of dc capacitors, respectively. However, they did not consider that there is a specific relationship in the calculation of the dc capacitance value necessary to compensate for the negative-sequence component at VSC ac terminals. Occasional thermal stresses and their influence on the capacitor lifetime can be evaluated using current ripple, but these analyses are not presented in this work.

Using (14), the current ripple i_d (Fig. 1) through the dc capacitor is given by

$$i_{d}=C\frac{d\tilde{v}_{dc}}{dt}=\frac{3V_{-}I_{+}}{V_{dc}}\cos\left(2\omega t+\phi_{v_{-}}+\phi_{i_{+}}+\pi\right), \tag{20}$$

and its rms value I_d is given by

$$I_{d}=\frac{3\sqrt{2}V_{-}I_{+}}{2V_{dc}}. \tag{21}$$

Considering the dc capacitance calculated using (19), the inertia constant of the VSC (in seconds) can be defined by

$$H_{c}=\frac{E_{c}}{S}=\frac{CV_{dc}^{2}}{2S}, \tag{22}$$

where S is the converter apparent power given by $\sqrt{3}V_{+}I_{+}$. This VSC inertia constant is analogous to the inertia constant of rotating electric machines [16]. Substituting (22) in (19), it is possible to verify how the inertia constant H_c influences the ripple voltage factor ε for a given unbalance factor δ, as follows

$$\varepsilon=\frac{3\delta V_{+}I_{+}}{2\omega H_{c}S}=\frac{\sqrt{3}\delta}{2\omega H_{c}}\cong\frac{2.3\delta}{H_{c}'}, \tag{23}$$

where, e.g., $\omega=2\pi(60)$ rad/s and $H_c'=H_c/1\times10^{-3}$ s.

Thus, in an unbalanced system, (23) shows that the ripple voltage factor ε is directly proportional to the voltage unbalance factor δ. Also, occurs that the larger the inertia constant H_c, the smaller the ripple voltage factor.

IV. VSC AC-Side Harmonic Currents Due to DC-Side Voltage Ripple

Considering the assumption 6 listed in the introduction and the system shown in Fig. 3, the three-phase voltage source is considered to have only positive-sequence component. The voltage at PCC is unbalanced due to unbalanced load configuration. The PLL [6], [17] is used to synchronize the VSC with the positive-sequence grid voltage component and a unified three-phase signal processor (UTSP) [11] is also used to detect and quantify the negative-sequence voltage at PCC.

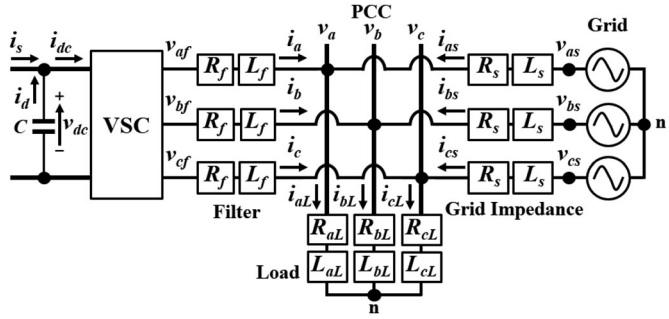

Fig. 3. A distribution power system considering an unbalanced voltage.

Assuming a VSC with PWM switching function F_{sw} [18], the a-phase voltage of the VSC ac-side terminal is given by

$$v_{af} = F_{sw} v_{dc}, \tag{24}$$

which, in expanded form, becomes:

$$v_{af} = F_1 v_{dc} \sin(\omega t) + v_{dc} \sum_{h}^{\infty} F_h \sin(\omega_h t), \tag{25}$$

where F_1 is the magnitude of the fundamental or desired component of the switching function, and F_h and ω_h are the higher-order harmonic magnitude and angular frequency, respectively, of the VSC PWM switching function. We consider that (i) the VSC has a current control loop, and (ii) the switching frequency is high enough to assume that the harmonic content due to PWM switching is eliminated by the coupling inductance L_f.

Thus, assuming all switching harmonics are ideally eliminated, the a-phase current on the VSC ac-side terminal, can be written as

$$i_a = M_1 v_{dc} \sin(\omega t + \phi_{i_+}), \tag{26}$$

where $M_1 v_{dc}$, in these operating conditions, represents $I_1 = M_1 V_{dc} = \sqrt{2} I_+$, the magnitude of the fundamental frequency current component. In this ideal operation $v_{dc} = V_{dc}$ (no dc voltage ripple), and M_1 represents the fundamental component of the switching function after the effect of VSC series impedance (VSC output filter).

Now, the VSC series impedance is considered to be designed basically to eliminate the high frequency PWM switching harmonics. Therefore, when there is ripple on the capacitor voltage v_{dc} at twice the line frequency, by using (5) and (18) in (26), it is possible to analyze the low-frequency harmonic component that appears on the VSC ac-side. These low-frequency current component harmonics due to the dc voltage ripple for three phases are given by (for detailed derivation see Appendix)

$$\begin{aligned} i_a = {} & \sqrt{2} I_+ \sin[(\omega t + \phi_{i_+})] \\ & + \frac{\varepsilon}{4} \sqrt{2} I_+ \sin\left[\left(\omega t + \phi_{v_-} + \frac{3\pi}{2}\right)\right] \\ & - \frac{\varepsilon}{4} \sqrt{2} I_+ \sin\left[\left(3\omega t + \phi_{v_-} + 2\phi_{i_+} + \frac{3\pi}{2}\right)\right]. \end{aligned} \tag{27}$$

$$\begin{aligned} i_b = {} & \sqrt{2} I_+ \sin\left[\left(\omega t + \phi_{i_+}\right) - \frac{2\pi}{3}\right] \\ & + \frac{\varepsilon}{4} \sqrt{2} I_+ \sin\left[\left(\omega t + \phi_{v_-} + \frac{3\pi}{2}\right) + \frac{2\pi}{3}\right] \\ & - \frac{\varepsilon}{4} \sqrt{2} I_+ \sin\left[\left(3\omega t + \phi_{v_-} + 2\phi_{i_+} + \frac{3\pi}{2}\right) - \frac{2\pi}{3}\right] \end{aligned} \tag{28}$$

$$\begin{aligned} i_c = {} & \sqrt{2} I_+ \sin\left[\left(\omega t + \phi_{i_+}\right) + \frac{2\pi}{3}\right] \\ & + \frac{\varepsilon}{4} \sqrt{2} I_+ \sin\left[\left(\omega t + \phi_{v_-} + \frac{3\pi}{2}\right) - \frac{2\pi}{3}\right] \\ & - \frac{\varepsilon}{4} \sqrt{2} I_+ \sin\left[\left(3\omega t + \phi_{v_-} + 2\phi_{i_+} + \frac{3\pi}{2}\right) + \frac{2\pi}{3}\right]. \end{aligned} \tag{29}$$

Amplitudes of second and third terms of current from (27)–(29) are directly proportional to the ripple voltage factor ε. These additional terms are generated by the oscillating voltage component $\tilde{v}_{dc}$ given by (18), which is generated due to the real power oscillating component $\tilde{p}$, present on the ac-side of the VSC. It is very important to note that, due to the dc voltage ripple, there are two undesirable current components in (27)–(29): a fundamental negative sequence component and a third-order positive-sequence harmonic component. Normally, third-order harmonic components generated by converters are of zero-sequence type and do not flow in three-wire circuits. However, here they are of positive-sequence type.

In [6], the VSC dc-side voltage control tends to eliminate the dc oscillating voltage, however disregarding what happens with the ac-side current due to this control. So, it is important to analyze what happens when the VSC controls the real power p to keep zero oscillating voltage across the dc capacitor (i.e., $v_{dc} = V_{dc}$). In fact, the dc voltage ripple can be eliminated if the VSC is controlled in such a way that the real power in its ac terminals has no oscillating component. Therefore, considering the instantaneous power formulation [9] and using (1) in the $\alpha\beta$-axes (v_α and v_β) and considering $p = \overline{p}$, the real currents in $\alpha\beta$ reference frame in the VSC are given by

$$\begin{bmatrix} i_\alpha \\ i_\beta \end{bmatrix} = \frac{1}{v_\alpha^2 + v_\beta^2} \begin{bmatrix} v_\alpha & v_\beta \\ v_\beta & -v_\alpha \end{bmatrix} \begin{bmatrix} \overline{p} \\ 0 \end{bmatrix}. \tag{30}$$

For simplicity, the imaginary power q is assumed to be equal to zero. The instantaneous currents in the abc reference frame on the VSC ac side are obtained by

$$\begin{bmatrix} i_a \\ i_b \\ i_c \end{bmatrix} = \sqrt{\frac{2}{3}} \begin{bmatrix} 1 & 0 \\ -\frac{1}{2} & \frac{\sqrt{3}}{2} \\ -\frac{1}{2} & -\frac{\sqrt{3}}{2} \end{bmatrix} \begin{bmatrix} i_\alpha \\ i_\beta \end{bmatrix}. \tag{31}$$

Thus, considering (30) the case of ac-side three-phase voltage with the unbalance factor given by δ, and using (31), the low

frequency current harmonic components due to the unbalanced voltage at PCC for the three phases are given by

$$\begin{aligned} i_a = D\{&(1-\delta c)\left[\sin\left(\omega t + 2\phi_{v_+} - \phi_{i_+}\right)\right. \\ &\left. + \sin\left(\omega t + \phi_{i_+}\right)\right] \\ &+ (\delta - c)\left[\sin\left(\omega t + \phi_{v_+} + \phi_{v_-} - \phi_{i_+}\right)\right. \\ &\left. + \sin\left(\omega t - \phi_{v_+} + \phi_{v_-} + \phi_{i_+}\right)\right] \\ &+ (c)\left[\sin\left(3\omega t + 3\phi_{v_+} + \phi_{v_-} - \phi_{i_+}\right)\right. \\ &\left. + \sin\left(3\omega t + \phi_{v_+} + \phi_{v_-} + \phi_{i_+}\right)\right] \\ &+ (\delta c)\left[\sin\left(3\omega t + 2\phi_{v_+} + 2\phi_{v_-} - \phi_{i_+}\right)\right. \\ &\left. + \sin\left(3\omega t + 2\phi_{v_-} + \phi_{i_+}\right)\right]\} \end{aligned} \tag{32}$$

$$\begin{aligned} i_b = D\Bigg\{&(1-\delta c)\left[\sin\left(\omega t + 2\phi_{v_+} - \phi_{i_+} - \frac{2\pi}{3}\right)\right. \\ &\left. + \sin\left(\omega t + \phi_{i_+} - \frac{2\pi}{3}\right)\right] \\ &+ (\delta - c)\left[\sin\left(\omega t + \phi_{v_+} + \phi_{v_-} - \phi_{i_+} + \frac{2\pi}{3}\right)\right. \\ &\left. + \sin\left(\omega t - \phi_{v_+} + \phi_{v_-} + \phi_{i_+} + \frac{2\pi}{3}\right)\right] \\ &+ (c)\left[\sin\left(3\omega t + 3\phi_{v_+} + \phi_{v_-} - \phi_{i_+} - \frac{2\pi}{3}\right)\right. \\ &\left. + \sin\left(3\omega t + \phi_{v_+} + \phi_{v_-} + \phi_{i_+} - \frac{2\pi}{3}\right)\right] \\ &+ (\delta c)\left[\sin\left(3\omega t + 2\phi_{v_+} + 2\phi_{v_-} - \phi_{i_+} + \frac{2\pi}{3}\right)\right. \\ &\left. + \sin\left(3\omega t + 2\phi_{v_-} + \phi_{i_+} + \frac{2\pi}{3}\right)\right]\Bigg\} \end{aligned} \tag{33}$$

$$\begin{aligned} i_c = D\Bigg\{&(1-\delta c)\left[\sin\left(\omega t + 2\phi_{v_+} - \phi_{i_+} + \frac{2\pi}{3}\right)\right. \\ &\left. + \sin\left(\omega t + \phi_{i_+} + \frac{2\pi}{3}\right)\right] \\ &+ (\delta - c)\left[\sin\left(\omega t + \phi_{v_+} + \phi_{v_-} - \phi_{i_+} - \frac{2\pi}{3}\right)\right. \\ &\left. + \sin\left(\omega t - \phi_{v_+} + \phi_{v_-} + \phi_{i_+} - \frac{2\pi}{3}\right)\right] \\ &+ (c)\left[\sin\left(3\omega t + 3\phi_{v_+} + \phi_{v_-} - \phi_{i_+} + \frac{2\pi}{3}\right)\right. \\ &\left. + \sin\left(3\omega t + \phi_{v_+} + \phi_{v_-} + \phi_{i_+} + \frac{2\pi}{3}\right)\right] \\ &+ (\delta c)\left[\sin\left(3\omega t + 2\phi_{v_+} + 2\phi_{v_-} - \phi_{i_+} - \frac{2\pi}{3}\right)\right. \\ &\left. + \sin\left(3\omega t + 2\phi_{v_-} + \phi_{i_+} - \frac{2\pi}{3}\right)\right]\Bigg\} \end{aligned} \tag{34}$$

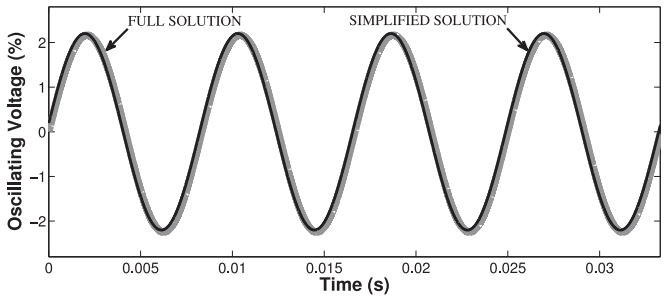

Fig. 4. DC oscillating voltage using full (10) and simplified (15) solutions, considering $H_c = 1$ ms and $\delta = 7.6\%$.

with

$$D = \frac{\sqrt{2}I_+}{(1+\delta^2)\left[2 - 8c^2\cos^2\left(2\omega t + \phi_{v_+} + \phi_{v_-}\right)\right]}, \tag{35}$$

and

$$c = \frac{\delta}{1+\delta^2}. \tag{36}$$

The currents given in (32)–(34) turn into three-phase balanced currents if there is no ac voltage unbalance ($\delta = 0$). However, if unbalance is present, these currents present undesirable components like the fundamental negative-sequence (e.g., a-phase I_{a-}) and the third-order harmonic components of positive (I_{a3+}) and negative sequences (I_{a3-}).

V. Analytical Studies and Discussion

In this section, the VSC model is implemented in the MATLAB/Mathworks software in order to illustrate the steady state behavior. It is considered that the frequency of the system is constant and the voltage variation in each phase is within $\pm 5\%$ of the rated voltage. The unbalance factor δ is usually smaller than 2% [19].

The VSC (Fig. 3) is based on PWM with sinusoidal current-mode control. Initially, the VSC ac-side power is considered as an average value $\overline{p}$ added to an oscillating component $\tilde{p}$, which allows to calculate the VSC dc capacitance (VSC inertia constant) and the noncharacteristic ac harmonics with the objective of keeping these harmonics below given limits. In a second step, the VSC is controlled such that $\tilde{p} = 0$ [6], determining the negative- and positive-sequence third order harmonic (3ω) that appears at the VSC ac side.

The dc-side oscillating voltage is calculated from the complete solution (10) and from the simplified solution given by (15), considering $H_c = 1$ ms and $\delta = 7.6\%$, as shown in Fig. 4. It can be seen that the difference between both oscillating voltages (obtained from (10) and (15)) is considerably low (below 0.01%), which validates the approximation used to derive (15) and confirms the oscillating dc voltage at 2ω. The considered value of inertia constant, $H_c = 1$ ms, is usual in STATCOM [4] and results in a large dc voltage ripple. In an old STATCOM [20] whenever the unbalance factor reaches a given limit, its operation is blocked to avoid this excessive dc ripple.

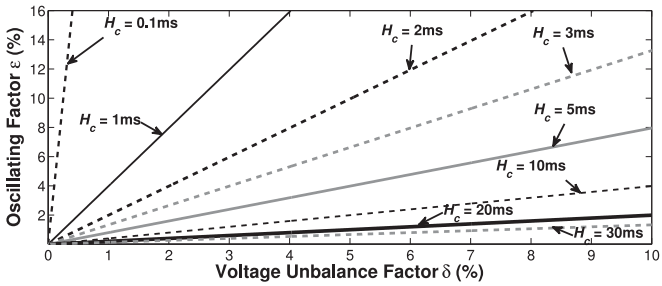

Fig. 5. Variation of oscillating factor ε as a function of δ for several inertia constant values (generally, STATCOM uses $H_c < 10$ ms and VSC for renewable sources uses $H_c > 10$ ms).

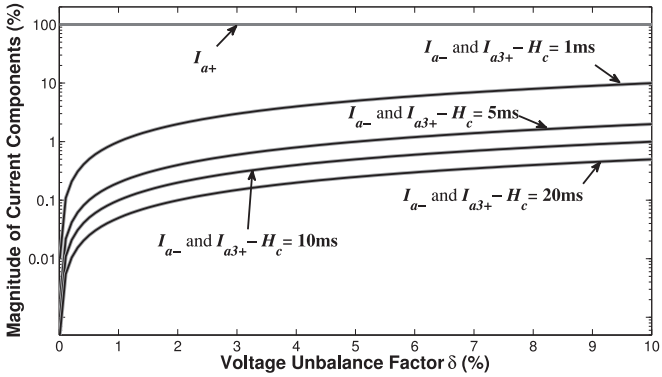

Fig. 6. Effect of unbalance factor δ at PCC in the VSC ac-side current (e.g., a-phase) for several inertia constant values H_c.

The relation between the oscillation factor ε and the unbalance factor δ, is obtained for different values of the inertia constant (H_c varying from 0.1 ms to 30 ms), as shown in Fig. 5. It can be noticed that a VSC with a small dc capacitor, (e.g., $H_c = 0.66$ ms [12]), may have a relatively large dc oscillating voltage factor ε even if the unbalance factor δ is within its normal 2% limit range required by the power quality standards [19]. A constant of inertia in this range is used in equipment such as STATCOM [4] and it may be a problem in real applications. The use of larger inertia constants (above 20 ms) results in a limited dc voltage oscillation. Indeed, the use of a larger dc capacitor seems to be the best solution to keep ε below a given value (e.g., 2%). However, it is important to note that a larger dc capacitor affects the dynamic response of the VSC [6], as well as the cost and size of equipment.

It is worth mentioning that it was assumed that the converter control strategy is usually designed to generate a balanced three-phase fundamental current component only. However, the instantaneous oscillating real power $\tilde{p}$ arises due to the interaction between the negative-sequence voltage and this positive-sequence current. This power $\tilde{p}$ oscillates at 2ω and, in turn, it causes the double frequency dc oscillating voltage on the dc capacitor.

It can be noticed that the values of the fundamental negative sequence and the third-order harmonic positive sequence rise when the voltage unbalance factor δ increases, as shown in Fig. 6. Such components reach 1% of magnitude of the

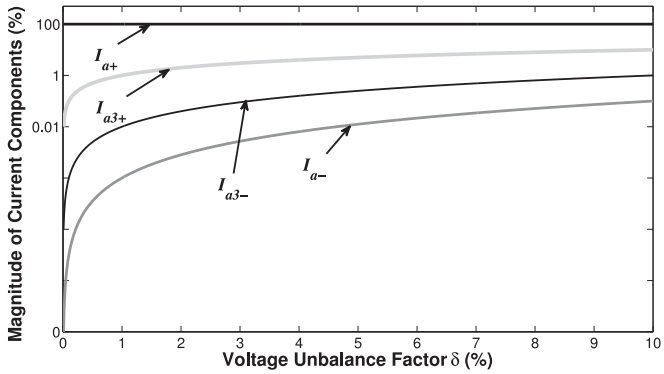

Fig. 7. Effect of unbalanced voltage at PCC on the VSC ac-side current (e.g. a-phase) as a function of the voltage unbalance factor δ for constant real power on the VSC ac side.

fundamental component (I_{a+}) for $\delta = 10\%$, even for $H_c = 10$ ms. This situation shows that δ must be less than 10%, at least if it is intended to maintain I_{a-} and I_{a3+} below 1%, considering $H_c = 10$ ms. However, considering $H_c = 1$ ms, the components reach 1% of magnitude of the fundamental component for $\delta = 1\%$, i.e., only for a low distortion factor value.

The dc voltage oscillation makes the VSC ac-side currents become unbalanced (negative-sequence component) and distorted (positive-sequence third harmonic). However, it is clear that increasing the value of H_c can reduce this dc voltage oscillation.

Unbalanced voltage effects in the normalized ac current amplitude (a-phase) of the VSC are shown in Fig. 6 for $H_c = 1, 5, 10$ and 20 ms. This figure shows that, for inertia constants greater than 10 ms, the magnitude of the fundamental negative-sequence current and the positive-sequence third harmonic components are both kept below 1%.

It is worth to notice that if the control suggested in [6] to eliminate the dc capacitor voltage oscillation is used, the ac currents have to be given by (32)–(34). The real power, in this case, is constant (only $\overline{p}$ exists) on the ac-side of the VSC and no oscillation is present in the dc capacitor. However, the fundamental positive- and negative-sequence currents and the third-order harmonic positive- and negative-sequence current characteristics appear (Fig. 7) due to the constant power on VSC under unbalanced condition. In this case, the magnitudes of the current does not depend on the inertia constant H_c, provided that the VSC PWM control is able to keep real power constant. For three-phase VSCs, it is clear that the magnitudes of these non-characteristic harmonics are not significant and this technique may be a good solution to maintain these harmonics below the given limits [8]. However, the third-order positive-sequence harmonic (I_{a3+}) is approximately 1% of the fundamental component and, when added to other characteristic harmonics, may result in problems to comply with the regulations.

VI. Simulation Results

A three-phase three-wire grid (Fig. 3) is modeled in the PSCAD/EMTDC software [21], in order to validate the

TABLE I
ELECTRICAL PARAMETERS OF THE SYSTEM

Parameter	Nomenclature	Value
Power Rating	S	10 (kVA)
Grid Frequency	f	60 (Hz)
VSC Switching Frequency	f_{sw}	5 (Hz)
Average dc Voltage	V_{dc}	600 (V)
Grid Voltage	$V_{as} = V_{bs} = V_{cs}$	127 (Vrms)
a-Phase Load	R_{aL}	1.18 (Ω)
a-Phase Load	L_{aL}	1.79 (mH)
b- and c-Phase Load	$R_{bL} = R_{cL}$	2.18 (Ω)
b- and c-Phase Load	$L_{bL} = L_{cL}$	2.79 (mH)
VSC Filter	R_f	48.25 (mΩ)
VSC Filter	L_f	1.28 (mH)
Grid Resistance	R_s	0.19 (Ω)
Grid Inductance	L_s	0.39 (mH)

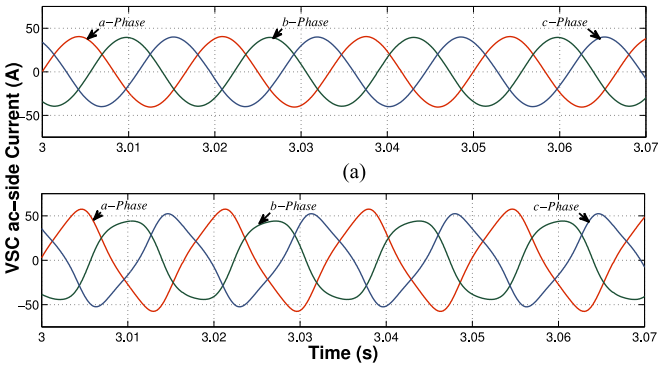

Fig. 8. VSC ac-side currents, using $\delta = 2.2\%$ (a) and $\delta = 26\%$ (b) for $H_c = 1$ ms.

analytical study of the VSC in the time-domain simulation. The VSC PSCAD/EMTDC model was composed using the built-in models of the IGBTs and diodes, using the switching frequency at 5 kHz. The VSC is based on PWM with current-mode control (Fig. 2). The electrical parameters of the system are presented in Table I.

This analysis initially considers $H_c = 1$ ms, $\delta = 2.2\%$ and that the VSC (PSCAD/EMTDC model) dc side is connected to an alternative energy source which supplies only constant average ac power, producing constant current.

The response of the VSC ac-side currents, considering unbalance factor $\delta = 2.2\%$ (load impedance at Table I) and $\delta = 26\%$ (load impedance: $R_{aL} = 0.11\ \Omega, L_{aL} = 0.14$ mH, $R_{bL} = R_{cL} = 2.18\ \Omega, L_{bL} = L_{cL} = 2.79$ mH) for inertia constant $H_c = 1$ ms, is illustrated in Fig. 8. Using (23), the oscillation factor ε goes to 5% and 59.8%, respectively. These operating conditions (steady state after 3 seconds) lead to unbalanced sinusoidal voltage (amplitude and phase).

The increase of the inertia constant can lead to the attenuation of the VSC ac-side current distortion due to dc-side ripple. The third harmonic component can be kept below 1%, using (27) (e.g. $I_{3+} = \varepsilon/4$) to calculate the new value of oscillating factor for $\delta = 26\%$, which leads to ripple voltage factor $\varepsilon = 4\%$.

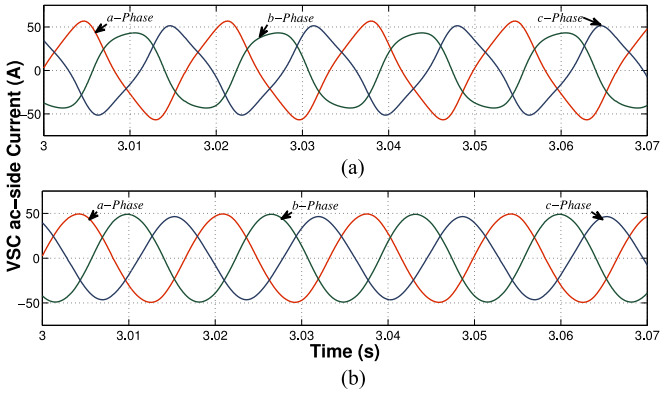

Fig. 9. VSC ac-side currents, using $H_c = 1$ ms (a) and $H_c = 15$ ms (b) for $\delta = 26\%$.

TABLE II
COMPARISON WITH ANALYTICAL APPROACH

H_c (ms)	$\delta(\%)$	THD(%)	I_{3+} (%)	I_{3+} (%)*
1.0	0.0	0.0	0.0	0.0
1.0	2.0	1.2	0.9	1.2
1.0	9.0	5.1	4.0	5.0
1.0	26.0	12.8	10.0	14.0
15.0	26.0	5.5	1.7	1.0

*Analytical model results

With this value, it is possible to obtain the new inertia constant $H_c = 15$ ms from (23).

The responses of the VSC ac-side currents from PSCAD/EMTDC, considering the unbalance factor $\delta = 26\%$ for the inertia constants $H_c = 1$ ms (a) and $H_c = 15$ ms (b), are illustrated in Fig. 9.

Table II shows the results from time-domain simulation (PSCAD/EMTDC) considering balanced and unbalanced VSC ac-side voltages. When a higher value of unbalance factor occurs, the VSC is turn off [20] or a dc capacitor with higher capacitance is used on VSC dc side [8].

The VSC ac-side currents are balanced and without harmonics if the unbalance factor $\delta = 0$, as shown in Fig. 10(a). Notice, in Fig. 10(b), that the waveform harmonic distortion is THD $= 5.1\%$ with a relatively high unbalance factor ($\delta = 9\%$).

VII. CONCLUSIONS

This paper presented the ac-side current behavior obtained from an analytical model proposed by the authors for a three-phase three-wire VSC connected to a weak and unbalanced power system. This model presents an accurate analytical formulation for understanding and calculating the generation of the dc-side voltage ripple at twice the line frequency as well as the fundamental frequency current of negative sequence and a third-order harmonic of positive and negative sequences. These problems may affect the power quality indices and the lifetime of components, such as dc capacitors. The analytical model derived for three-phase systems can be applied to single-phase

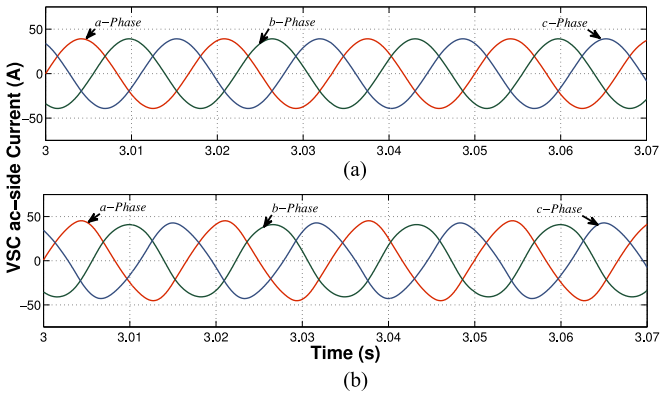

Fig. 10. VSC ac-side currents, using $\delta = 0\%$ (a) and $\delta = 9\%$ (b) for $H_c = 1$ ms.

systems and is especially helpful in the calculation of dc-side capacitors for this type of VSC. The amplitude of the noncharacteristic current harmonic components due to unbalanced voltage condition was analyzed.

The results based on the proposed analytical model of VSC are in good agreement with those obtained from time-domain simulation.

Appendix
Derivation of VSC AC Currents

The derivation of i_a, i_b and i_c in (27)–(29) can be done by first considering only the VSC ac-side a-phase current. Using (5) and (26), the a-phase current results in:

$$i_a = M_1 v_{dc} \sin(\omega t + \phi_{i_+}) = M_1 [V_{dc} + \tilde{v}_{dc}] \sin(\omega t + \phi_{i_+}), \tag{37}$$

by substituting $\tilde{v}_{dc}$ given in (18), we have:

$$i_a = M_1 \left[V_{dc} + \frac{\varepsilon V_{dc}}{2} \sin(2\omega t + \phi_{v_-} + \phi_{i_+} + \pi) \right] \sin(\omega t + \phi_{i_+}), \tag{38}$$

which can be rewritten as

$$\begin{aligned} i_a &= M_1 V_{dc} \sin(\omega t + \phi_{i_+}) \\ &\quad + M_1 V_{dc} \frac{\varepsilon}{2} \sin(2\omega t + \phi_{v_-} + \phi_{i_+} + \pi) \sin(\omega t + \phi_{i_+}) \end{aligned} \tag{39}$$

The first term in the right hand side of (39) represents the "desirable" current and the second term represents the "undesirable" components as defined in [22]. Equation (39) can be rewritten as:

$$\begin{aligned} i_a &= M_1 V_{dc} \sin(\omega t + \phi_{i_+}) \\ &\quad + \frac{\varepsilon}{2} M_1 V_{dc} \left[\frac{1}{2} \cos(2\omega t + \phi_{v_-} + \phi_{i_+} + \pi - \omega t - \phi_{i_+}) \right. \\ &\quad \left. - \frac{1}{2} \cos(2\omega t + \phi_{v_-} + \phi_{i_+} + \pi + \omega t + \phi_{i_+}) \right] \end{aligned} \tag{40}$$

or

$$\begin{aligned} i_a &= M_1 V_{dc} \sin(\omega t + \phi_{i_+}) \\ &\quad + \frac{\varepsilon}{4} M_1 V_{dc} \sin\left(\omega t + \phi_{v_-} + \frac{3\pi}{2}\right) \\ &\quad - \frac{\varepsilon}{4} M_1 V_{dc} \sin\left(3\omega t + \phi_{v_-} + 2\phi_{i_+} + \frac{3\pi}{2}\right). \end{aligned} \tag{41}$$

Now, by similarity, we can derive the expressions for VSC ac-side b- and c-phase currents:

$$\begin{aligned} i_b &= M_1 V_{dc} \sin\left[(\omega t + \phi_{i_+}) - \frac{2\pi}{3}\right] \\ &\quad + \frac{\varepsilon}{4} M_1 V_{dc} \sin\left[\left(\omega t + \phi_{v_-} + \frac{3\pi}{2}\right) + \frac{2\pi}{3}\right] \\ &\quad - \frac{\varepsilon}{4} M_1 V_{dc} \sin\left[\left(3\omega t + \phi_{v_-} + 2\phi_{i_+} + \frac{3\pi}{2}\right) - \frac{2\pi}{3}\right] \end{aligned} \tag{42}$$

and

$$\begin{aligned} i_c &= M_1 V_{dc} \sin\left[(\omega t + \phi_{i_+}) + \frac{2\pi}{3}\right] \\ &\quad + \frac{\varepsilon}{4} M_1 V_{dc} \sin\left[\left(\omega t + \phi_{v_-} + \frac{3\pi}{2}\right) - \frac{2\pi}{3}\right] \\ &\quad - \frac{\varepsilon}{4} M_1 V_{dc} \sin\left[\left(3\omega t + \phi_{v_-} + 2\phi_{i_+} + \frac{3\pi}{2}\right) + \frac{2\pi}{3}\right]. \end{aligned} \tag{43}$$

In equations (41), (42) and (43) we can define $I_1 = M_1 V_{dc} = \sqrt{2} I_+$ and rewrite the three-phase currents as given in (27)–(29).

References

[1] J.-W. Moon, J.-W. Park, D.-W. Kang, and J.-M. Kim, "A control method of HVDC-modular multilevel converter based on arm current under the unbalanced voltage condition," *IEEE Trans. Power Del.*, vol. 30, no. 2, pp. 529–536, Apr. 2015.

[2] V. Blasko and V. Kaura, "A new mathematical model and control of a three-phase ac-dc voltage source converter," *IEEE Trans. Power Electron.*, vol. 12, no. 1, pp. 116–123, Jan. 1997.

[3] M. Singh, V. Khadkikar, A. Chandra, and R. K. Varma, "Grid interconnection of renewable energy sources at the distribution level with power-quality improvement features," *IEEE Trans. Power Del.*, vol. 26, no. 1, pp. 307–315, Jan. 2011.

[4] C. A. C. Cavaliere, E. H. Watanabe, and M. Aredes, "Multi-pulse STATCOM operation under unbalanced voltages," *Proc. IEEE Power Eng. Soc. Winter Meeting*, 2002, pp. 567–572.

[5] A. von Jouanne and B. Benerjee, "Assessment of voltage unbalance," *IEEE Trans. Power Del.*, vol. 16, no. 4, pp. 782–790, Oct. 2001.

[6] A. Yazdani and R. Iravani, "A unified dynamic model and control for the voltage sourced converter under unbalanced grid conditions," *IEEE Trans. Power Del.*, vol. 21, no. 3, pp. 1620–1629, Jul. 2006.

[7] H. Wang and F. Blaabjerg, "Reliability of capacitors for dc-link applications in power electronic converters–An overview," *IEEE Trans. Ind. Appl.*, vol. 50, no. 5, pp. 3569–3578, Sep./Oct. 2014.

[8] C. F. Nascimento, E. H. Watanabe, A. B. Dietrich, R. F. S. Dias, and O. Diene, "Non-characteristic harmonics and dc side capacitor calculation in VSC connected to a distribution system with unbalanced voltage," *Proc. 24th IEEE Int. Symp. Ind. Electron.*, 2015.

[9] H. Akagi, E. H. Watanabe, and M. Aredes, *Instantaneous Power Theory and Applications to Power Conditioning*. Piscataway, NJ, USA: IEEE/Wiley, 2007.

[10] N. A. Ahmed, A. K. Al-Othman, and M. R. AlRashidi, "Development of an efficient utility interactive combined wind/photovoltaic/fuel cell power system with MPPT and DC bus voltage regulation," *Elect. Power Syst. Res.*, vol. 81, no. 5, pp. 1096–1106, May 2011.

[11] H. Karimi, A. Yazdani, and R. Iravani, "Negative-sequence current injection for fast islanding detection of a distributed resource unit," *IEEE Trans. Power Electron.*, vol. 23, no. 1, pp. 298–307, Jan. 2008.
[12] B. Singh and J. Solanki, "A comparison of control algorithms for DSTATCOM," *IEEE Trans. Ind. Electron.*, vol. 56, no. 7, pp. 2738–2745, Jul. 2009.
[13] J. G. Hwang, P. W. Lehn, and M. Winkelnkemper, "Control of grid connected AC-DC converters with minimized DC link capacitance under unbalanced grid voltage condition," *Proc. Eur. Conf. Power Electron. Appl.*, 2007, pp. 1–10.
[14] P. T. Krein, R. S. Balog, and M. Mirjafari, "Minimum energy and capacitance requirements for single-phase inverters and rectifiers using a ripple port," *IEEE Trans. Power Electron.*, vol. 27, no. 11, pp. 4690–4698, Nov. 2012.
[15] Z. Qin, H. Wang, F. Blaabjerg, and P. C. Loh, "Investigation into the control methods to reduce the dc link capacitor ripple current in a back-to-back converter," *Proc. IEEE Energy Convers. Congr. Expo.*, 2014, pp. 203–210.
[16] M. Hagiwara, K. Wada, H. Fujita, and H. Akagi, "Dynamic behavior of a 21-level BTB-based power-flow controller under single-line-to-ground fault conditions," *IEEE Trans. Ind. Appl.*, vol. 43, no. 5, pp. 1379–1387, Sep./Oct. 2007.
[17] L. G. B. Rolim, D. R. da Costa Jr., and M. Aredes, "Analysis and software implementation of a robust synchronizing PLL circuit based on the pq theory," *IEEE Trans. Ind. Electron.*, vol. 53, no. 6, pp. 1919–1926, Dec. 2006.
[18] C. Marouchos, "The switching function: Analysis of power electronic circuits," *IET Circuits, Devices and Systems*, ser. Devices and Systems Series. London, U.K., 2006.
[19] "IEEE recommended practice for monitoring electric power quality," IEEE Standard 1159, 2009.
[20] S. Mori, K. Matsuno, T. Hasegawa, S. Ohnishi, M. Takeda, M. Seto, S. Murakami, and F. Ishiguro, "Development of a large static VAr generator using self-commutated inverters for improving power system stability," *IEEE Trans. Power Syst.*, vol. 8, no. 1, pp. 371–377, Feb. 1993.
[21] Y. Zhou, D. Jiang, J. Guo, P. Hu, and Y. Liang, "Analysis and control of modular multilevel converters under unbalanced conditions," *IEEE Trans. Power Del.*, vol. 28, no. 4, pp. 1986–1995, Oct. 2013.
[22] L. Gyugyi and B. R. Pelly, *Static Power Frequency Changers: Theory, Performance and Application*. New York, USA: Wiley, 1976.

Claudionor F. Nascimento received the B.Sc. degree in electrical engineering from Sao Paulo State University (UNESP), Brazil, in 1992, and the M.Sc. and the Ph.D. degrees in electrical engineering from University of Sao Paulo (USP), Sao Paulo, Brazil, in 2003 and 2007, respectively.

Currently, he is an Associate Professor at Federal University of Sao Carlos (UFSCar).

Edson H. Watanabe received the B.Sc. degree in electronic engineering and the M.Sc. degree in electrical engineering from the Federal University of Rio de Janeiro (UFRJ), Rio de Janeiro, Brazil, in 1975 and 1976, respectively, and the D.Eng. degree from the Tokyo Institute of Technology, Tokyo, Japan, in 1981.

From 1981 to 1994, he was an Associate Professor with COPPE/UFRJ, where he has been a Professor since 1994. Currently, he is the Director of COPPE/UFRJ.

Dr. Watanabe was admitted to the National Order of Scientific Merit (2005), is a member of the National Academy of Engineering (2013), and member of the Brazilian Academy of Science (2014). He was the recipient of the 2013 IEEE PES Nari Hingorani FACTS Award.

Oumar Diene received the Eng., M.Sc., and D.Sc. degrees in electrical engineering from the Federal University of Rio de Janeiro (UFRJ), Rio de Janeiro, Brazil, in 2002, 2004, and 2008, respectively.

Currently, he is an Associate Professor at UFRJ.

Alvaro B. Dietrich received the B.Sc., M.Sc., and Ph.D. degrees in electrical engineering from the University of Sao Paulo, Sao Paulo, Brazil, in 1997, 2000, and 2005, respectively.

Currently, he is an Associate Professor at Federal University of ABC (UFABC).

Alessandro Goedtel received the B.S. degree in electrical engineering from Federal University of Rio Grande do Sul (UFRGS), Brazil, in 1997, the M.Sc. degree in industrial engineering from UNESP, Brazil, in 2003, and the Ph.D. degree in electrical engineering from the University of Sao Paulo, São Paulo, Brazil, in 2007.

Currently, he is an Assistant Professor at Federal Technological University of Parana (UTFPR).

Johan J. C. Gyselinck received the M.Sc. degree in electrical and mechanical engineering and the Doctor of Applied Sciences degree from Ghent University, Ghent, Belgium, in 1991 and 2000, respectively.

Currently, he is an Associate Professor at Université Libre de Bruxelles (ULB), Brussels, Belgium.

Robson F. S. Dias received the B.Sc. degree in electrical engineering from Federal University of Para (UFPA), Brazil, in 2002, and the Ph.D. degree in electrical engineering from the Federal University of Rio de Janeiro (UFRJ), Rio de Janeiro, Brazil, in 2008.

Currently, he is an Associate Professor at UFRJ.